Post-Print of an Accepted Manuscript on the Laboratory of Turbulent Flows Website

Experiments in Fluids manuscript No.
(will be inserted by the editor)

A Fuzzy Cluster Method for Turbulent/Non-Turbulent Interface Detection

Khaled Younes, Bradley Gibeau, Sina Ghaemi, Jean-Pierre Hickey

Received: date / Accepted: date

Abstract A turbulent/non-turbulent interface detection method is proposed based on fuzzy clustering of the instantaneous streamwise velocity field. The fuzzy cluster method overcomes the limitations of standard detection methods by removing the user bias in thresholding and window selection and not relying on the calculation of mean flow properties. The robust detection algorithm is applied to three experimental wall-bounded turbulent flows, and it is found to compare favorably against existing interface identification methods.

Keywords Turbulent/Non-Turbulent Interface · Detection algorithm · Turbulent boundary layer

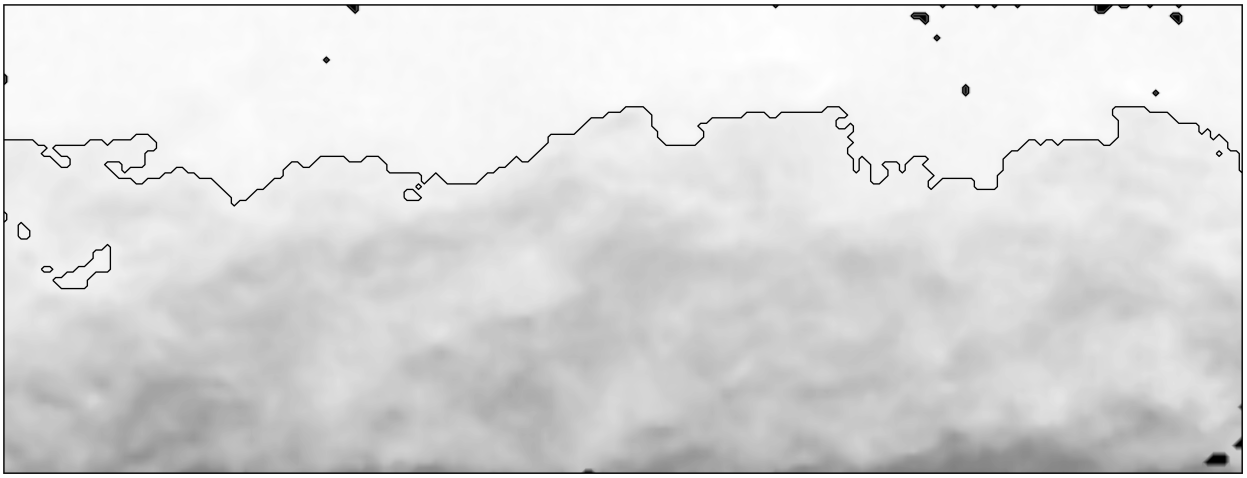

Khaled Younes, Jean-Pierre Hickey
Department of Mechanical and Mechatronics Engineering, University of Waterloo, 200 University Ave West, Waterloo, Ontario, Canada
Bradley Gibeau, Sina Ghaemi
Department of Mechanical Engineering, University of Alberta, 116 St & 85 Ave, Edmonton, Alberta, Canada

1 Introduction

External turbulent flows, such as wakes, jets, and boundary layers, are characterized by a corrugated, three-dimensional interface that delineates the regions of active turbulence from the irrotational flow in the free stream. The so-called turbulent/non-turbulent interface (TNTI) plays a key role in the kinematics of turbulence—it is the location where entrainment of non-turbulent flow takes place and mixing occurs. Hence, accurately detecting it is of fundamental importance.

Numerically, the TNTI is trivially identified using thresholding methods based on vorticity (Bisset et al., 2002), enstrophy (Borrell and Jiménez, 2016), or by probability density functions constructed with the velocity profile (Wu et al., 2019). The ease of detection in numerical simulations is tributary to: (1) the relatively low-Reynolds number imposed by computational limitations, and (2) the low level of numerical noise present in the free stream. Both contribute to a crisp delineation of the turbulent and non-turbulent regions in numerical simulations.

From an experimental perspective, however, detecting the TNTI is not as straightforward, especially in wall-bounded flows. This is in part due to the generally high-Reynolds number encountered in such flows, but also, as noted by Reuther and Kähler (2018), due to a trade-off between noise and spatial resolution in Particle Image Velocimetry (PIV) and Particle Tracking Velocimetry (PTV) techniques. The often large level of experimental noise measured in the free stream translates into significant errors in the gradient calculations. This renders any vorticity-based thresholding techniques too difficult to apply in experimental settings.

With that said, the three methods commonly employed in experimental TNTI detection are fraught with limitations. The turbulent kinetic energy (TKE) method of Chauhan et al. (2014) uses a windowing approach based on the turbulent fluctuations to determine the rotational and irrotational regions of the flow. As the determination of the turbulent fluctuations relies on an accurate measurement of the mean flow profile, the method is only applicable to a statistically steady, quiescent flow. The homogeneity method (HM) alleviates this drawback by utilizing a local mean flow velocity instead. However, this makes the method particularly sensitive to the sampling window and yields an overly smooth TNTI (Reuther and Kähler, 2018). Finally, the particle density method (PDM), which is largely thought to be the most accurate and robust, implicitly assumes the possibility of local seeding. In cases where local seeding is not possible or the boundary layer development is not known *a priori*, the method cannot be applied.

To this end, a reliable TNTI detection method, based on a fuzzy clustering algorithm, is proposed in this paper. The algorithm overcomes the aforementioned limitations by acting directly on the velocity field, eliminating the need to compute any mean flow properties or perform flow seeding. We show that the method can be applied to robustly detect the TNTI in a variety of experimental wall-bounded flows. Moreover, it can be readily extended to encompass three-dimensional flows, as done in Fan et al. (2019).

2 Method description

A brief summary of the fuzzy cluster algorithm, also known as fuzzy C-means (FCM), is given herein. A detailed description of the method, as applied to the identification of the uniform momentum zones (UMZ), can be found in Fan et al. (2019).

The FCM takes as input a sequence of M measurements from a single snapshot, represented by $\vec{\phi} = \{\phi_1 \dots \phi_M\}$ where ϕ can be any experimentally determined or numerically simulated scalar variable, as well as a user-defined number of clusters, N. After initialization, the algorithm computes the centroid for each cluster, c, which corresponds to the characteristic mean of the subset. Then, it classifies the data using a distance-from-the-mean metric, the Euclidean norm, and updates the classification labels such that the cost function is minimized:

$$cost(C_1, \dots, C_N) = min \sum_{j=1}^{N} \sum_{i \in C_j} \Pi_{ij} ||\phi_i - c_j||^2, \qquad (1)$$

where C_q corresponds to the q-th cluster and Π_{ij} is the probability of clustering ϕ_i in cluster C_j. By definition, $0 \leq \Pi_{ij} \leq 1$. The process is repeated until convergence, at which point the centroids of the clusters are stationary with respect to a preset error threshold, ϵ. Commonly, the error threshold is selected such that $|C_k^{new} - C_k^{old}| \leq \varepsilon < \epsilon$, where ε is a small number. Upon convergence, the contour separating the clusters is identified to be the TNTI.

The algorithm is developed in Python and is publicly available at `https://git.uwaterloo.ca/jphickey/tnti`. It differs from that proposed by Fan et al. (2019) in that multiple successive clusterings are utilized in order to maximize the fuzzy partition coefficient (FPC). The FPC is analytically defined as:

$$\text{FPC} = \frac{1}{N} \sum_{j=1}^{N} \sum_{i=1}^{M} \Pi_{ij}^2, \qquad (2)$$

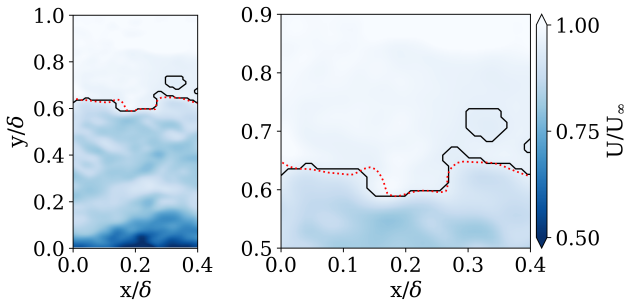

Fig. 1 TNTI detection with: (——) FCM and (·····) TKE as applied on the experimental data of Gibeau and Ghaemi (2021). The threshold for TKE is $k_{th} = 0.35$; streamwise velocity contours are shown.

and it is an indicator for how well the data is described by the fuzzy clustering model; it is normalized such that a value of unity represents a perfect solution.

3 Results

To highlight the versatility of the method, the FCM approach is applied to detect the TNTI for experimental (PIV) measurements of turbulent boundary layer flows, and its performance is assessed by comparison with the TKE method. For all the cases studied, the algorithm is initialized randomly, the variable used for clustering is the streamwise velocity component, U, and two user-defined clusters, $N = 2$, are selected. In addition, the convergence criterion is set to $\varepsilon = 10^{-5}$, and two successive clusterings are employed. The cluster count and number of iterative clusterings were optimally selected by studying various combinations and choosing the values that maximize the classification agreement, i.e., that give the highest FPC. An FPC well over 90% was computed for each investigated case.

The FCM algorithm is tested on three different experimental data sets. First, the PIV data of Gibeau and Ghaemi (2021) from the University of Alberta at $Re_\tau = 2600$, where Re_τ is the friction Reynolds number. Figure 1 plots the TNTI as detected by the FCM algorithm and the TKE method, where the threshold for TKE, k_{th}, is determined by the procedure outlined in Chauhan et al. (2014). Excellent agreement is obtained between the two methods. The TNTI generated by FCM traces that from TKE, apart from a pocket in the free stream. These detached patches are typically encountered in TNTI detection and can be discounted when considering the continuous interface.

Second, the classical zero pressure gradient flat boundary layer flow of Adrian et al. (2000) at $Re_\theta = 7705$ (high-Re case), where Re_θ is the Reynolds number based on the momentum thickness. The results from both

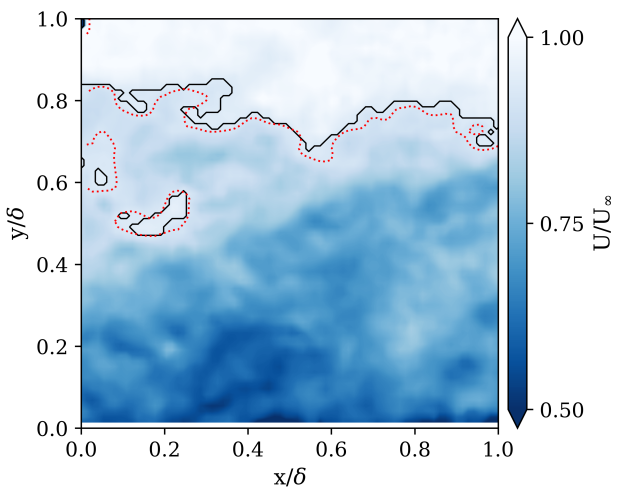

Fig. 2 TNTI detection with: (——) FCM and (·····) TKE as applied on the high-Re experimental data of Adrian et al. (2000). The threshold for TKE is $k_{th} = 0.68$; streamwise velocity contours are shown.

methods are overlaid and presented in Figure 2. As can be seen, the algorithm yields a TNTI that closely resembles that detected by the traditional TKE approach.

Third, the low-Re case of Adrian et al. (2000) at $Re_\theta = 1015$, shown in Figure 3. Again, the TNTI detected by FCM matches reasonably well with that produced by TKE. While the results in Figures 1–3 are in agreement, we note that arriving to the optimal TKE thresholds took several attempts via trial-and-error. On the other hand, the FCM algorithm converged rapidly with no extra user input. This is the chief advantage of FCM, and it gives us confidence that the method is generalizable for experimental data.

To provide a statistical measure of the agreement, the intermittency factor γ, defined as the ratio of the flow that is turbulent at a given y-location, is computed in Figure 4 for the experimentally determined TNTI. Two main remarks can be made. First, the intermittency factor in all cases closely follows the expected error function behavior, starting from unity at the wall and dropping to a very low value (≈ 0.05) at the edge of the boundary layer. Second, the profiles from both methods collapse similarly with a maximum discrepancy of 6%. The discrepancy is more pronounced in the high-Re case of Adrian et al. (2000); this is attributed to the narrow field of view in the wall-normal direction, at the upper edge of the boundary layer, and the lower number of PIV snapshots available for statistical convergence. The mean location of the TNTI, y_i, is also highlighted—the TNTI is well within the boundary layer ($y_i = 0.61\delta$ for Gibeau and Ghaemi (2021) and $y_i = 0.7\delta$ for Adrian et al. (2000)); this is in line with the observations of Chauhan et al. (2014).

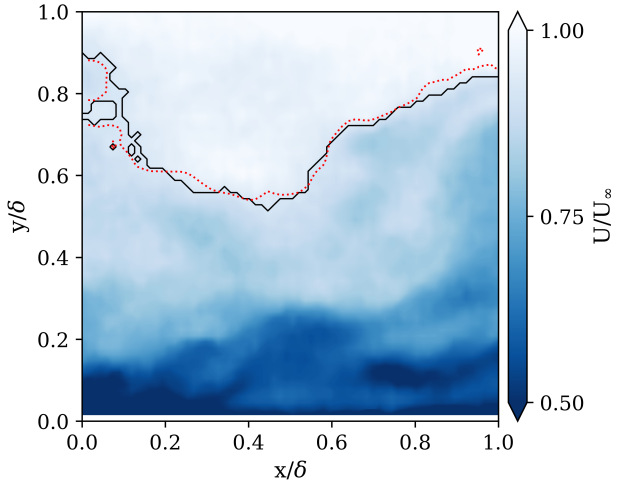

Fig. 3 TNTI detection with: (——) FCM and (·····) TKE as applied on the low-Re experimental data of Adrian et al. (2000). The threshold for TKE is $k_{th} = 0.57$; streamwise velocity contours are shown.

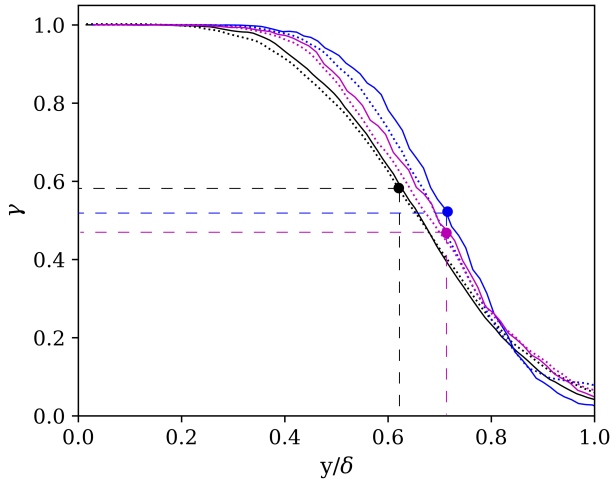

Fig. 4 Intermittency profile for the experimental data set of (——) Gibeau and Ghaemi (2021), calculated with 1,000 snapshots, and Adrian et al. (2000) (——) high-Re and (——) low-Re, calculated with 45 snapshots each. Markers and dashes indicate the coordinates of the mean TNTI as computed with FCM. Dotted lines show the profiles from TKE.

Finally, the conditionally-averaged streamwise velocity, $\langle U \rangle$, is calculated in close proximity to the TNTI. The profiles are displayed in Figure 5, where a sharp step-change and an inflection point are apparent across the turbulent/non-turbulent interface. This validates the TNTI location detected by FCM and corroborates the evidence of a shear-like 'superlayer' at the TNTI, as first proposed by Corrsin and Kistler (1955).

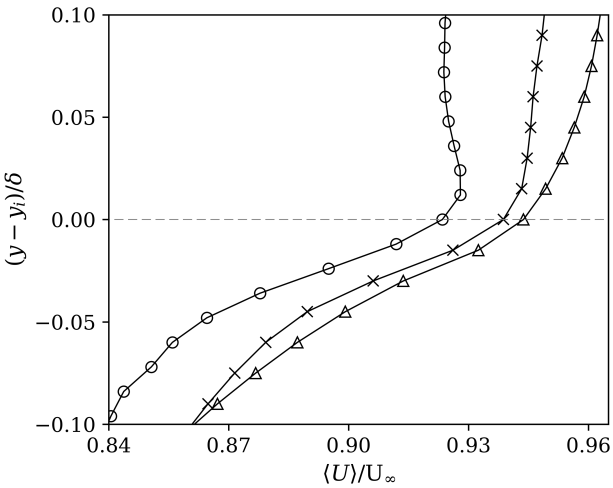

Fig. 5 Conditionally-averaged velocity profile as a function of distance from the TNTI. (○) Gibeau and Ghaemi (2021) with 1,000 snapshots; Adrian et al. (2000) (×) high-Re; (△) low-Re with 45 snapshots each.

4 Conclusion

A TNTI detection method is proposed based on a fuzzy cluster means algorithm. The approach overcomes the windowing, thresholding, and seeding limitations associated with current prominent detection methods, without requiring the computation of the mean flow velocity. It is tested against three experimental data sets, and it is shown to perform comparably to TKE. The algorithm is proven to be robust, versatile, and convenient for TNTI detection in wall-bounded flows, but it is applicable for any other free-shear flow. The method can also be extended to identify three-dimensional interfaces. An open-source code is available and all the data within this paper is provided for full reproducibility.

References

Adrian RJ, Meinhart CD, Tomkins CD (2000) Vortex organization in the outer region of the turbulent boundary layer. J Fluid Mech 422:1–54, DOI 10.1017/S0022112000001580

Bisset D, Hunt J, Rogers M (2002) The turbulent/non-turbulent interface bounding a far wake. J Fluid Mech 451:383–410, DOI 10.1017/S0022112001006759

Borrell G, Jiménez J (2016) Properties of the turbulent/non-turbulent interface in boundary layers. J Fluid Mech 801, DOI 10.1017/jfm.2016.430

Chauhan K, Philip J, de Silva C, Hutchins N, Marusic I (2014) The turbulent/non-turbulent interface and entrainment in a boundary layer. J Fluid Mech 742:119–151, DOI 10.1017/jfm.2013.641

Corrsin S, Kistler AL (1955) Free-stream boundaries of turbulent flows. Tech. rep., Washington, DC

Fan D, Xu J, Yao MX, Hickey JP (2019) On the detection of internal interfacial layers in turbulent flows. J Fluid Mech 872:198–217, DOI 10.1017/jfm.2019.343

Gibeau B, Ghaemi S (2021) Low- and mid-frequency wall-pressure sources in a turbulent boundary layer. Submitted to J Fluid Mech

Reuther N, Kähler CJ (2018) Evaluation of large-scale turbulent/non-turbulent interface detection methods for wall-bounded flows. Exp Fluids 59(121), DOI 10.1007/s00348-018-2576-2

Wu X, Wallace JM, Hickey JP (2019) Boundary layer turbulence and freestream turbulence interface, turbulent spot and freestream turbulence interface, laminar boundary layer and freestream turbulence interface. Phys Fluids 31(4), DOI 10.1063/1.5093040